Effects of Multi-Axial Mechanical Stress on Loss Characteristics of Electrical Steel Sheets and Interior Permanent Magnet Machines

Katsumi Yamazaki[1], Hirofumi Mukaiyama[1], and Laurent Daniel[2]

[1]Department of Electrical, Electronic, and Computer Engineering, Chiba Institute of Technology, Narashino 275-0016, Japan
[2]Group of Electrical Engineering Paris, 91192 Cedex, France

In this paper, we investigate the effects of multi-axial mechanical stress on eddy current and hysteresis losses in electrical steel sheets used for rotating machines. First, the variation of these losses with the multi-axial stress is confirmed by material experiments. From the results, appropriate and useful mechanical-electromagnetic modeling for loss analysis of rotating machines is discussed. Finally, the proposed modeling is applied to the combined electromagnetic field and stress analyses of an interior permanent magnet machine to reveal the effects of multi-axial stress on the rotor core loss, which is directly related to the thermal demagnetization of permanent magnets. It is clarified that both the hysteresis loss and the eddy current loss including excess loss depend on the multi-axial stress. As a consequence, the rotor core loss of interior permanent magnet machine increases by the stress caused by centrifugal force.

Index Terms—**Finite-element method (FEM), losses, permanent magnet machines, stress.**

I. Introduction

IT IS well known that mechanical compressive stress significantly affects the magnetic behavior of electrical steels with significant consequences on the performance of rotating machines. The most famous effect is the increase in core loss at stator yokes by shrink fitting of housings. In this case, the directions of both the major component of principal stress and the magnetic field at the yoke are nearly in circumferential direction. Therefore, this core loss increase is often estimated by material experiments, in which a uniaxial stress is imposed along the flux direction.

On the other hand, large tensile stress is often generated at the rotor cores of interior permanent magnet synchronous machines (IPMSMs) according to the centrifugal forces worked on magnets and cores [1]. In the rotor of this motor, the direction of the flux considerably varies with position in the core. As a consequence, the direction of the magnetic field is not always parallel to the highest principal stress, rather in right angle to the stress in some cases. Therefore, the investigation of the effects of multi-axial stress on the core loss is needed for the accurate estimation of rotor core loss, which is directly related to the PM thermal demagnetization.

The effect of the multi-axial stress on the total core loss in electrical steel sheets has been investigated in [2]. However, the effects on each loss component, i.e., the eddy current and hysteresis losses, have not been clarified yet. The detailed variation of these losses with the multi-axial stress should be clarified for the development of loss calculation method for rotating machines because the ratio of these losses to the total core loss considerably varies with machine operating conditions.

From these viewpoints, in this paper, the variation of these losses with the multi-axial stress is confirmed by material experiments. Then, appropriate and useful mechanical-electromagnetic modeling for loss analysis of rotating machines is discussed. Finally, the proposed modeling is applied to the combined electromagnetic field and stress analyses of an IPMSM to reveal the effects of multi-axial stress on the rotor core loss.

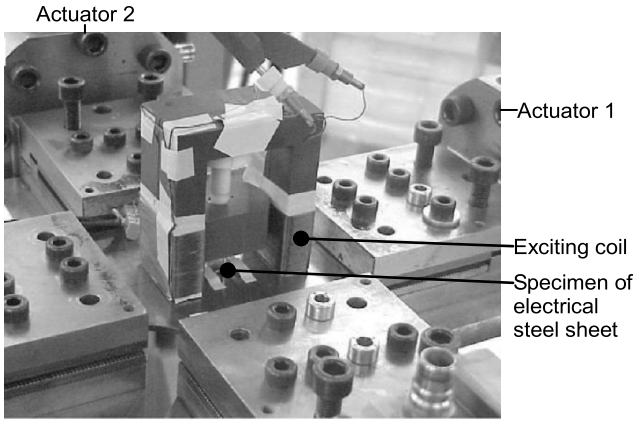

Fig. 1. Experimental system for effect of multi-axial stress [2].

II. Basic Experiments for Multi-Axial Stress Effects

A. Experimental System

Fig. 1 shows the experimental system used in [2], in which arbitrary 2-axial stress (σ_1, σ_2) can be imposed on the specimen of an electrical steel sheet by the actuators noted 1 and 2. The magnetic field is applied along the direction of the force produced by actuator 1. The specimen is an electrical steel sheet with 3% silicon. The magnetic field H is measured by a calibrated H-coil placed at the surface of the specimen, whereas the flux density B is measured by using a needle-B sensor.

Fig. 2 shows the examples of measured hysteresis loops, which include the effect of the eddy current loss and the excess

Manuscript received June 27, 2017; accepted September 19, 2017. Corresponding author: K. Yamazaki (e-mail: yamazaki.katsumi@it-chiba.ac.jp).
Color versions of one or more of the figures in this paper are available online at http://ieeexplore.ieee.org.
Digital Object Identifier 10.1109/TMAG.2017.2757531

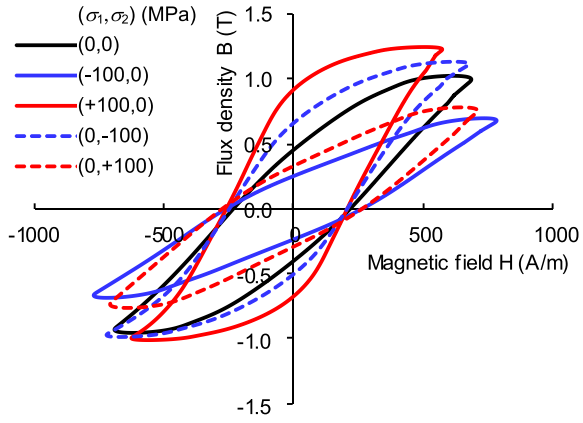

Fig. 2. Examples of measured hysteresis loops.

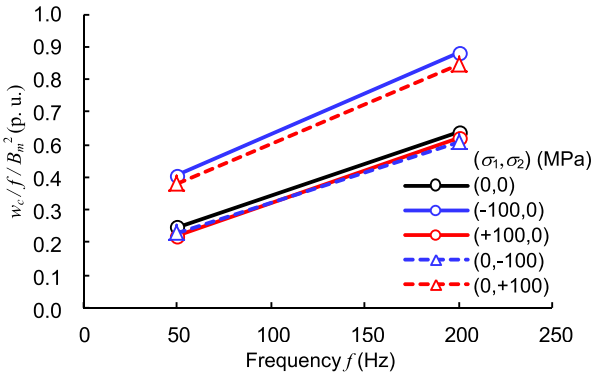

Fig. 3. Determination of core loss coefficients.

loss. It is observed that the loop depends on both σ_1 and σ_2. From these results, the core loss per weight w_c is obtained, as follows:

$$w_c = \frac{f}{D}\oint H dB \tag{1}$$

where f is the frequency and D is the density.

B. Loss Separation

It is considered that the effects of the stress on the core loss vary with both frequency f and flux density B. However, vast number of measurement should be carried out to obtain the variation with σ_1, σ_2, f, and B. From this viewpoint, a well-known approximation [3] is applied to the experimental results, as follows:

$$w_c \cong K_e(\sigma_1,\sigma_2) f^2 B_m^2 + K_h(\sigma_1,\sigma_2) f B_m^2 \tag{2}$$

where K_e and K_h are the eddy current and hysteresis loss coefficients, respectively, B_m is the amplitude of the hysteresis loop. The effect of excess loss is included in K_e. This approximation is acceptable when f is relatively low and harmonics are negligible [3]. In this case, K_e and K_h can be obtained by the slope and intercept of Fig. 3, respectively. As a result, the eddy current and hysteresis losses can be separated.

Fig. 4 shows the eddy current and hysteresis losses separated by the measured losses at 50 and 200 Hz. It is revealed that both the eddy current and hysteresis losses are affected by multi-axial stress. These losses become maximum when the compressive (minus) σ_1 and tensile (plus) σ_2 are imposed. This is an original result that is first obtained in this paper.

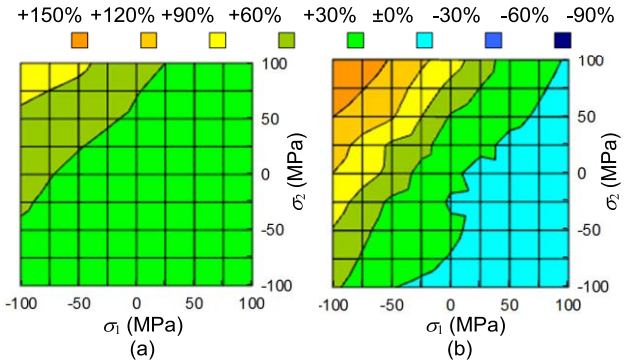

Fig. 4. Measured variation in losses with multi-axial stress. (a) Eddy current loss. (b) Hysteresis loss.

III. Equivalent Stress for Loss Calculation

A. Equivalent Stress Expressions

The experiments explained in Section II cannot be always carried out for many kinds of electrical steel sheets. To obtain the approximated multi-axial stress effects, the single axial equivalent stress σ_{eq} has been proposed.

In [4], following expression was derived under the assumption that the same macroscopic magneto-elastic energy leads to same characteristics of the magnetic material

$$\sigma_{\mathrm{eq}} = \frac{3}{2}\vec{h}\cdot\boldsymbol{s}\cdot\vec{h} \tag{3}$$

where $\vec{h}$ is the unit vector along the magnetic field direction, $\boldsymbol{s}$ is the deviatoric part of the stress tensor expressed from σ_1 and σ_2. It is assumed that the variation in core loss with uniaxial σ_{eq} along the magnetic field direction is identical to that with multi-axial σ_1 and σ_2. Therefore, the effect of the multi-axial stress can be estimated only by (3) and one set experimental results, in which a uniaxial stress is simply imposed along the flux direction.

In [5], the expression (3) was expanded to the following one by using basic considerations on the evolution of magnetic domain structure under stress:

$$\sigma_{\mathrm{eq}}^{C} = \frac{1}{K}\ln\left\{\frac{2\exp(K\vec{h}\cdot\boldsymbol{s}\cdot\vec{h})}{\exp(K\vec{t}_1\cdot\boldsymbol{s}\cdot\vec{t}_1)+\exp(K\vec{t}_2\cdot\boldsymbol{s}\cdot\vec{t}_2)}\right\} \tag{4}$$

where $\vec{t}_1$ and $\vec{t}_2$ are the unit vectors that are perpendicular to the magnetic field, K is a material parameter reflecting the effect of magnetic domains, as follows [5]:

$$K = \frac{9}{2}\frac{\chi_0\lambda_m}{\mu_0 M_s^2} \tag{5}$$

where χ_0 is the initial susceptibility, λ_m is the maximal magnetostriction, μ_0 is the vacuum permeability, and M_s is the saturation magnetization. In the case of the measured electrical steel sheet, K is estimated to be 2.7×10^{-8} (m^3/J).

The expressions (3) and (4) are derived from different levels of physics. The first one was tailored for anhysteretic magnetization while the second was extended to consider hysteresis effect. The mathematical relationship between (3) and (4) has not been discussed yet. Therefore, let us consider the case when K is very small. In this case, expression (4)

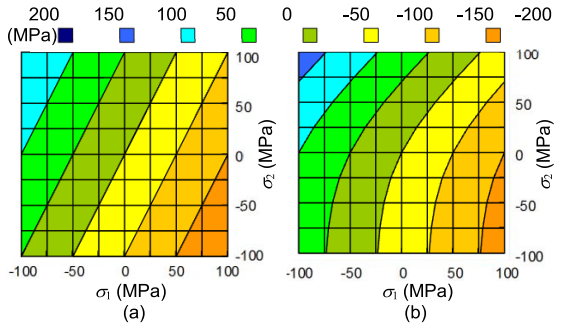

Fig. 5. Variation in equivalent stresses with multi-axial stress. (a) $\sigma_{\rm eq}(\sigma_1, \sigma_2)$. (b) $\sigma_{\rm eq}^{C}(\sigma_1, \sigma_2)$.

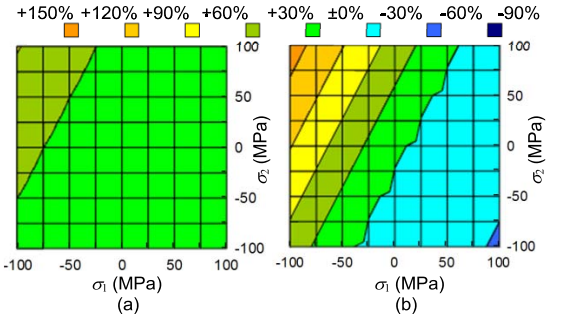

Fig. 6. Calculated losses by measured $W(\sigma_1, 0)$ and $\sigma_{\rm eq}(\sigma_1, \sigma_2)$ by (3). (a) Eddy current loss. (b) Hysteresis loss.

becomes

$$\lim_{K\to 0}\sigma_{\rm eq}^{C} \approx \frac{K\vec{h}\cdot\boldsymbol{s}\cdot\vec{h}}{K} - \frac{1}{K}\ln\left\{1+\frac{K\vec{t_1}\cdot\boldsymbol{s}\cdot\vec{t_1}+K\vec{t_2}\cdot\boldsymbol{s}\cdot\vec{t_2}}{2}\right\}$$
$$\approx \vec{h}\cdot\boldsymbol{s}\cdot\vec{h} - \frac{1}{K}\frac{K\vec{t_1}\cdot\boldsymbol{s}\cdot\vec{t_1}+K\vec{t_2}\cdot\boldsymbol{s}\cdot\vec{t_2}}{2}$$
$$= \frac{3}{2}\vec{h}\cdot\mathbf{s}\cdot\vec{h} = \sigma_{\rm eq}. \qquad (6)$$

It is mathematically proved that $\sigma_{\rm eq}^{c}(4)$ tends toward $\sigma_{\rm eq}$ (3) for particular material properties (low K). It can also be interpreted that when domain microstructure effects included in (4) are negligible, (3) can describe the effect of stress on hysteresis.

In the case of the experiments described in Section II, both $\sigma_{\rm eq}$ and $\sigma_{\rm eq}^{c}$ become the functions of (σ_1, σ_2), as shown in Fig. 5. Fig. 5 indicates that variation in $\sigma_{\rm eq}$ with (σ_1, σ_2) is linear, whereas that in $\sigma_{\rm eq}^{C}$ is nonlinear.

B. Approximated Loss Calculation by Equivalent Stress

Figs. 6 and 7 show the losses calculated by the equivalent stresses. Fig. 8 also shows the calculated losses extracted from Figs. 6 and 7, i.e., the losses when only $\sigma_2$that is perpendicular to the flux is imposed. In these figures, the losses are calculated only from the experimental losses on the horizontal axis in Fig. 4 $W(\sigma_1, 0)$ and the pure theoretical results of $\sigma_{\rm eq}$ and $\sigma_{\rm eq}^{C}$ expressed by (3) and (4), respectively. It is confirmed that these results well express the measured eddy current and hysteresis losses in Fig. 4. In detail, the result by $\sigma_{\rm eq}$ slightly underestimates the effect of σ_2 as compared with that by $\sigma_{\rm eq}^{C}$, particularly when the tensile σ_2 is imposed, as shown in Fig. 8.

These results implies that the effect of the multi-axial stress on both the eddy current and hysteresis losses can be

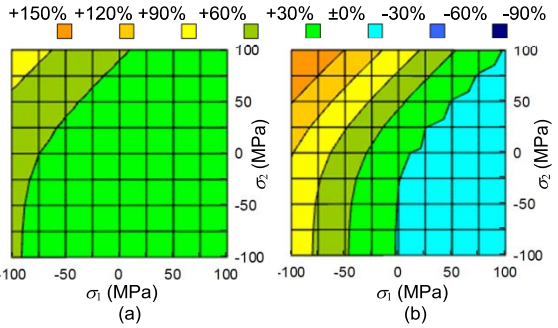

Fig. 7. Calculated losses by measured $W(\sigma_1, 0)$ and $\sigma_{\rm eq}^{C}(\sigma_1, \sigma_2)$ by (4). (a) Eddy current loss. (b) Hysteresis loss.

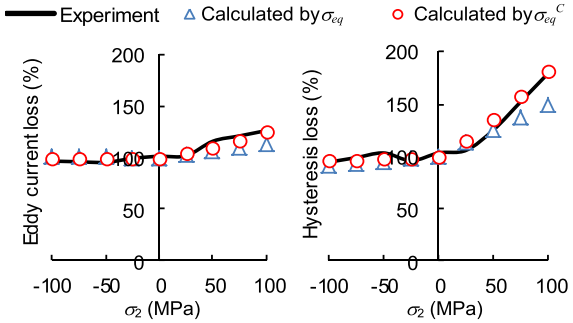

Fig. 8. Calculated losses when $\sigma_1 = 0$ and only σ_2 is imposed.

approximately estimated only from the experimental results with uniaxial stress imposed along the magnetic field, with the assist of the pure theoretical equivalent stresses. This estimation method must significantly contribute toward the loss estimation of rotating machines.

IV. Application to IPMSM

The above-mentioned equivalent stresses are applied to the combined electromagnetic field and stress analyses [1] for rotor core loss calculation of a 100 kW class IPMSM. The core characteristics with uniaxial stress are provided by the material manufacturer.

In the stress analysis, 2-D plane stress finite-element method (FEM) is used. On the other hand, the combination of main 2-D and post-1-D FEMs is applied to the electromagnetic field analysis. In this case, the reluctivity ν in both the 2-D and 1-D FEMs is determined by Newton–Raphson method due to the following expression [1]:

$$\nu(\sigma_1, \sigma_2, \boldsymbol{B}) = C_\nu(\sigma_{\rm eq}, |\boldsymbol{B}|)\nu_{\sigma 0}(|\boldsymbol{B}|) \qquad (7)$$

where C_ν is the reluctivity increase ratio that is obtained by the uniaxialstress experiment; $\nu_{\sigma_0}(|\boldsymbol{B}|)$ is the reluctivity when the mechanical stress is zero.

The core loss is obtained by the post-1-D FEM that considers the skin effect within the thickness of the electrical steel sheet [1] by using following expression:

$$w_c = \sum_{k=1}^{2}\{C_e(\sigma_{eq,k}, B_{{\rm max},k})w_{e,k,\sigma 0} + C_h(\sigma_{eq,k}, B_{{\rm max},k})w_{h,k,\sigma 0}\} \qquad (8)$$

where C_e and C_h are the increase ratios of eddy current and hysteresis losses obtained by the core material experiments, which correspond to the values on the horizontal axis

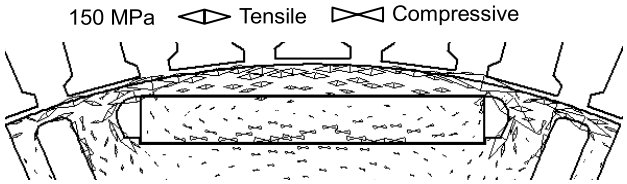

Fig. 9. Rotor stress distribution in IPMSM (10 000 r/min).

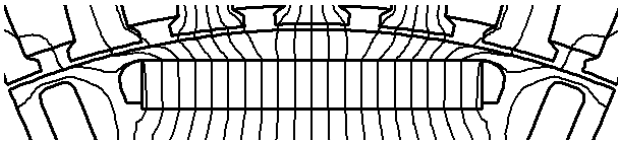

Fig. 10. Flux distribution in IPMSM (no-load).

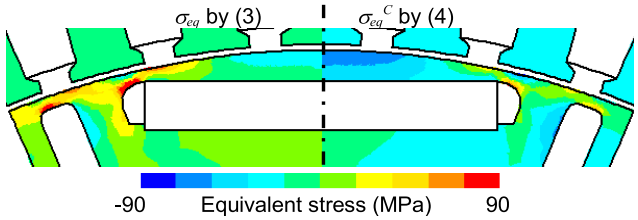

Fig. 11. Distribution of equivalent stresses (no-load, 10 000 r/min).

in Fig. 4(a) and (b) with uniaxial σ_1, respectively, $\sigma_{\mathrm{eq},1}$ and $\sigma_{\mathrm{eq},2}$ are the equivalent stresses for $\vec{h} = (1, 0)$ and $\vec{h} = (0, 1)$, respectively, $B_{\mathrm{max},1}$ and $B_{\mathrm{max},2}$ are the amplitude of flux-density components along the principal axes, respectively, and $w_{e,k,\sigma 0}$ and $w_{h,k,\sigma 0}$ are the eddy current and hysteresis losses caused by B_k when the mechanical stress is zero. The frequency and flux density dependence on the core loss is considered by this analysis with the core loss coefficients at low frequency in (2).

The application of σ_{eq} to (7) and (8) is already reported in [1]. In this paper, σ_{eq}^{C} by (4) is first applied instead of σ_{eq}. Then, the results are compared.

Figs. 9 and 10 show the principal stress vector and flux distributions at the maximum speed (10 000 r/min) under no-load condition. Large circumferential tensile stress caused by centrifugal force is observed at the rotor surface. This stress is almost in right angle to the magnetic field direction. This situation is almost identical to that of the plus σ_2 region in Fig. 8 in the basic experiment.

Fig. 11 shows the distribution of equivalent stresses σ_{eq} and σ_{eq}^{C} calculated from the result of Figs. 9 and 10. It is observed that the σ_{eq}^{C} tends to be negative as compared with σ_{eq}. The result of the σ_{eq}^{C} implies that the situation at the rotor surface shown in Figs. 9 and 10 is equivalent to that nearly 80 MPa compressive stress is imposed along the magnetic field direction. As a consequence, the rotor core loss increases.

Fig. 12 shows the rotor core losses calculated by the post-1-D FEM with the flux-density waveform obtained by the main 2-D FEM and the distribution of the equivalent stresses shown in Fig. 11. The result without the mechanical stress is also shown. The results at 2000 r/min are almost identical to each other because the centrifugal force is very small. On the other hand, at 10 000 r/min, the rotor core loss

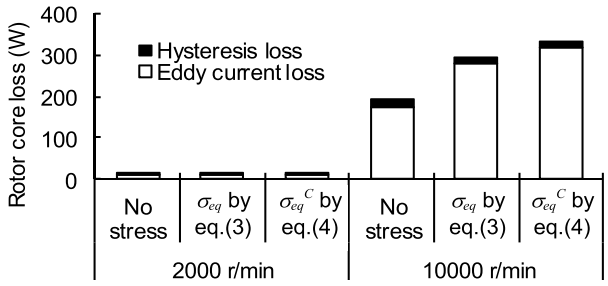

Fig. 12. Calculated rotor core loss of IPMSM at no load conditions.

without the stress is considerably underestimated as compared to that with the stress. This difference must not be negligible because the rotor loss, whose heat cannot be easily removed because of the existence of air gap, directly affects the thermal demagnetization of permanent magnets in IPMSMs. The result with σ_{eq}^{C} is larger than that with σ_{eq}. This tendency also appears in Fig. 8. Note that the increase in the eddy current loss in Fig. 12 is larger than that in Fig. 8 because the skin effect by the high-frequency slot harmonics is weakened according to an increase in ν by the stress.

V. Conclusion

The effects of multi-axial stress on eddy current and hysteresis losses in electrical steel sheets used for rotating machines are investigated. It is first revealed that both the eddy current and hysteresis losses are affected by the multi-axial stress. This effect is quantified separately by the proposed approach. The accuracies of the loss estimation method using two kinds of equivalent stresses are also confirmed by these experimental results. The mathematical relationship between these equivalent stresses is also demonstrated. It is validated that the equivalent stress that incorporates magnetic domain structure effects is more accurate than the simple one used in the previous papers for the estimation of core loss in rotating machines. Finally, the combined electromagnetic field and stress analyses of an IPMSM are carried out with the equivalent stresses. The importance of stress contribution to losses in IPMSM is confirmed, and satisfactorily estimated. From these experimental and calculated results, it can be stated that equivalent stress approach, particularly when considering magnetic domain structure effects, is effective for core loss estimation of rotating machines.

References

[1] K. Yamazaki and Y. Kato, "Iron loss analysis of interior permanent magnet synchronous motors by considering mechanical stress and deformation of stators and rotors," *IEEE Trans. Magn.*, vol. 50, no. 2, pp. 909–912, Feb. 2014.

[2] M. Rekik, O. Hubert, and L. Daniel, "Influence of a multiaxial stress on the reversible and irreversible magnetic behaviour of a 3%Si-Fe alloy," *Int. J. Appl. Electromagn. Mech.*, vol. 44, nos. 3–4, pp. 301–315, 2014.

[3] K. Yamazaki, A. Suzuki, M. Ohto, and T. Takakura, "Harmonic loss and torque analysis of high-speed induction motors," *IEEE Trans. Ind. Appl.*, vol. 48, no. 3, pp. 933–941, May/Jun. 2012.

[4] L. Daniel and O. Hubert, "An equivalent stress for the influence of multiaxial stress on the magnetic behavior," *J. Appl. Phys.*, vol. 105, no. 7, p. 07A313, 2009.

[5] M. Rekik, L. Daniel, and O. Hubert, "Equivalent stress model for magnetic hysteresis losses under biaxial loading," *IEEE Trans. Magn.*, vol. 50, no. 4, Apr. 2014, Art. no. 2001604.